Vis Comput (2010) 26: 761–768
DOI 10.1007/s00371-010-0444-z

ORIGINAL ARTICLE

Local albedo-insensitive single image dehazing

Jiawan Zhang · Liang Li · Guoqiang Yang · Yi Zhang · Jizhou Sun

Published online: 14 April 2010

Abstract In this paper, we present a new algorithm to remove haze from a single image. The proposed algorithm extracts transmission iteratively under the assumption that large-scale chromaticity variations are due to transmission while small-scale luminance variations are due to scene albedo. A nonlinear edge-preserving filter is introduced to incrementally refine subtle transmission map while still keeping sharp transmission map distinct. The algorithm is verified by both synthetic images and real-scene photographs. The results demonstrate that our method can produce transmission maps without being affected by the local albedo variations and, furthermore, recover haze-free images. On top of haze removal, several applications of the transmission map including refocusing and relighting are also implemented.

Keywords Image dehazing · Bilateral filter · Visibility restoration · Contrast enhancement

1 Introduction

The photographs we get in our daily life are easily plagued by the aerosols suspended in the medium, such as dust, mist, or fumes. The rays reflected by the objects' surfaces are not only attenuated by the existing aerosols but also blended with the *airlight* [11] when they reach the observers. Therefore, the quality of photographs taken in the foggy scenes are seriously degraded. They appear poor visibility and low vividness of the scene. One example scene is shown in Fig. 1(a).

J. Zhang (✉) · L. Li · G. Yang · Y. Zhang · J. Sun
School of Computer Science and Technology, Tianjin University, Tianjin, China
e-mail: yizhang@tju.edu.cn

(a) (b)

Fig. 1 Dehazing on single image. (**a**) Foggy image. (**b**) Dehazing results of our approach

The goal of dehazing algorithms is to recover color and details of scene from foggy image. There are many circumstances that accurate dehazing algorithms are needed. In computer vision, most existing applications assume that the radiance from a scene point to observer is not altered by airlight. However, the assumption is not practical in foggy scene since the light energy radiating from scene points is heavily scattered by atmosphere. Therefore, these applications will fail in bad weather conditions. In consumer photography, the images will be annoying with the presence of fog which decreases the contrast significantly. In aerial photography and satellite remote sensing, the photos are much more easily affected by aerosols. Even in clear days, the rays reflected by the ground will be scattered heavily when they pass through the earth's atmosphere, which will make image degraded.

Since the importance of the dehazing algorithm, much work has been done. Early in the dehazing field, the algorithms are mostly based on user interaction [14] or multiple images [16, 19]. Although these methods can significantly enhance the visibility, the labor-intensive or strict require-

ment on the inputs limits their applications. Dehazing from a single image has made great progress in recent years. It is a challenging work since the *airlight-albedo* ambiguity holds for every pixel and cannot be resolved independently [8]. In order to solve this ambiguity, a helpful assumption or prior is needed. We will summarize and compare the priors used by previous single image dehazing algorithms in Sect. 2.

Transmission map reflects the depth information of the scene and plays an essential role in visibility recovery. However, the estimation of transmission map is easily influenced by variations of local-albedo. For example, two thin objects in the same depth region may be assigned different transmission values if their surface albedos vary widely. The inaccuracy of transmission map will lead to color bias in the restored image.

In this paper we present a new method to recover haze-free image taking only one photograph as input. Based on the observation that the variations of depth are smooth in a local window, we propose the following assumption: the large-scale chromaticity variations in foggy image are due to depth, while small-scale variations are due to albedo. Then the blending model of degradation can be factored into a product of two components: one is called *transmission* which varies smoothly in a local window, and the other one is called *inverse-albedo* which changes correspondingly with scene albedo. Our objective is to separate these two components. For this purpose, Gaussian filter can be used. However, Gaussian filter may also make the edges of the transmission map blur. In order to refine the detailed transmission map, we propose an interactive bilateral filter that subtracts locally smooth variables from the initial image while preserving the edges. Our method can wipe off the influence of local albedo variations when estimating the transmission map. Once the transmission map is figured out, visibility can be recovered. Furthermore, we can use the depth information to create more visual effects on the restored image.

The remaining of this paper is organized as follows. In Sect. 2 we talk about the current available algorithms for dehazing from single image and the recent work on bilateral filter. Section 3 describes the degradation model we used in this paper. In Sect. 4 the detail of our algorithm is explained. The results and comparisons with other single image dehazing algorithms is shown in Sect. 5. Besides, Sect. 5 also includes additional applications based on restored images. Finally, we discuss our future work and conclude the paper in Sect. 6.

2 Related work

2.1 Single image dehazing

As we introduced in the previous section, dehazing from a single image is an ill-posed problem. So it is impossible to solve this intractable problem without any assumptions. There are many dehazing algorithms [9, 12, 20, 21] based on single image have been developed since Fattal [8]. All this works are based on one or more reasonable assumptions, physically or empirically.

Fattal [8] assumes that the transmission and the surface shading are locally uncorrelated. Under this assumption, Fattal first infers the transmission in the area affected by thin fog and then applies *Markov Random Field* on the transmission map in order to propagate the transmission to dense fog area and proceed with a statical smoothing. This approach is physically based and achieves good result. In most cases, this approach clarifies the airlight-albedo ambiguity and achieves good results. However, the method fails when all pixels on the image are affected by dense fog.

Tan's work [20] is based on two observations. One is that clear-day images have more contrast than images plagued by bad weather; The other is that the variations of airlight, which mainly depends on the distance of objects to the viewer, tend to be smooth. Therefore, the color and visibility can be recovered by maximizing the contrast in a local window of the foggy image. Although this approach may not be physically sound, the visual result is compelling.

He et al. [9] proposed Dark Channel Prior to solve the single image dehazing problem. It indicates that most local patches in haze-free outdoor images contain some pixels which have very low intensities in at least one color channel. By a minimum operator, the initial transmission map can be extracted from the foggy image. For a refinement purpose, soft matting is applies to the initial. Although the method is simple, the result is quite impressive.

Tarel [21] proposed a fast visibility restoration algorithm. The complexity of this algorithm is $\Theta(s_x \times s_y)$, where $s_x \times s_y$ is the resolution of the image. This method regards the airlight as a percentage between the local standard deviation and the local mean of the whiteness. This algorithm is proven to be faster than the other algorithms for most outdoor scene.

Kratz [12] uses the MAP model to solve the dehazing problem. The foggy image is modeled with factorial Markov Random Field in which the scene albedo and depth are two statically independent latent layers. The algorithm leverages albedo and depth information. Compared with other algorithms, it can generate more detailed depth map. However, some details are redundant.

2.2 Bilateral filter

The bilateral filter is a technique to smooth images while preserving edges. It can be traced back to Aurich's work [2]. Tomasi [22] gives it current name. The use of bilateral filtering has grown rapidly since it has been developed, and now it is ubiquitous in image-processing applications. It has been

used in denoising [1, 4, 13] for noise reduction, texture editing and relighting [17], tone management [5, 6], and stylization [23].

In parallel to applications, a wealth of theoretical studies [3, 5, 18] explained and characterized the bilateral filters behavior. The strengths and limitations of bilateral filtering are now fairly well understood. As a consequence, several extensions have been proposed [7].

3 Degradation model

3.1 Additive model

The formula widely used [8, 9, 12, 16, 21] in computer graphics and computer vision to describe the formation of the foggy image is an additive model:

$$\mathbf{I}(\mathbf{x}) = \mathbf{L}_\infty \rho(\mathbf{x}) e^{-\beta d(\mathbf{x})} + \left(1 - e^{-\beta d(\mathbf{x})}\right)\mathbf{L}_\infty, \tag{1}$$

where $\mathbf{I}(\mathbf{x})$ is the observed foggy image, $\rho(\mathbf{x})$ is called the scene albedo and expresses a ratio of total-reflected to incident by the scene point corresponding to pixel $\mathbf{x} = (x, y)$, $d(\mathbf{x})$ is the distance along the real-world ray corresponding to the pixel $\mathbf{x}$, $\mathbf{L}_\infty$ is atmosphere color, and β is the atmospheric attenuation coefficient. Both L_∞ and β are global constants over the whole image. $\rho(\mathbf{x})$ and $\mathbf{L}_\infty$ are three-channel vectors, the depth $d(\mathbf{x})$ is a scaler shared by three channels, and thus it should be actually viewed as $d(\mathbf{x}) = d(\mathbf{x})[1, 1, 1]$.

From the viewpoint of mathematics, the objective of single image dehazing is to solve $\rho(\mathbf{x})$, $d(\mathbf{x})$, and $\mathbf{L}_\infty$ from $\mathbf{I}(\mathbf{x})$. $\mathbf{L}_\infty \rho(\mathbf{x})$ is the fog-free image we desired.

The addend and the augend in (1) describe two mechanisms of the fog: one is called *direct attenuation*, and the other one is called *airlight*. Narasimhan's work [16] describes the two mechanisms in detail.

3.2 Multiplicative model

In this paper, we propose a multiplicative model by an algebraic rearrangement on (1). By defining $t(\mathbf{x}) = e^{-\beta d(\mathbf{x})}$, we get

$$1 - \frac{\mathbf{I}(\mathbf{x})}{\mathbf{L}_\infty} = t(\mathbf{x})(1 - \rho(\mathbf{x})). \tag{2}$$

$t(\mathbf{x})$ is called *transmission* and expresses the relative portion of light that managed to survive the entire path between the observer and the corresponding surface point in the scene without being scattered. $1 - \rho(\mathbf{x})$ is called *inverse-albedo* which changes correspondingly to albedo. We further define $\mathbf{B}(\mathbf{x}) \equiv 1 - \frac{\mathbf{I}(\mathbf{x})}{\mathbf{L}_\infty}$ and $\mathbf{C}(\mathbf{x}) \equiv 1 - \rho(\mathbf{x})$, and (2) is transformed as follows:

$$\mathbf{B}(\mathbf{x}) = t(\mathbf{x})\mathbf{C}(\mathbf{x}). \tag{3}$$

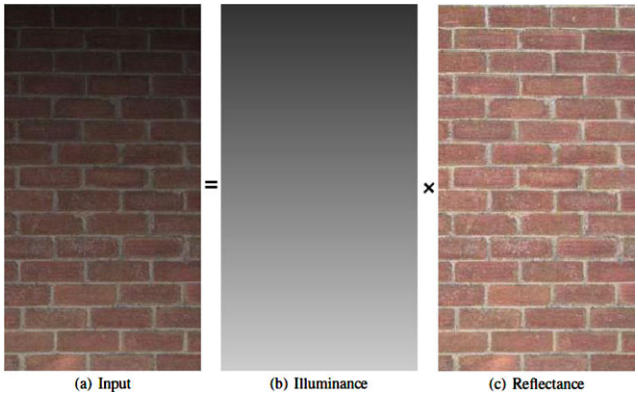

Fig. 2 The image decomposition

We call this model a multiplicative one. After estimating the atmosphere color $\mathbf{L}_\infty$ using the method introduced in Sect. 4.1, $\mathbf{B}(\mathbf{x})$ can be calculated from $\mathbf{I}(\mathbf{x})$. Then the dehazing task becomes separating the two components from the observed image.

The separation process utilizes the characteristic of the transmission and the inverse-albedo. First, we think about the characteristic of the transmission. The transmission is a continuous function of depth. Although there are discontinuities in depth map, most of the time the variations of depth are smooth [20]. So the variations of transmission are also smooth. In other words, the variations of transmission are large-scale. As to inverse-albedo, its variations are small-scale comparing to the transmission's. So the following assumption is reasonable: *large-scale intensity variations in* $\mathbf{B}(\mathbf{x})$ *are due to the transmission, and small-scale intensity variations are due to inverse-albedo*. In Sect. 4 we will the separation process based on this assumption in detail.

To well understand the transmission and the inverse-albedo, we can regard transmission as illuminance and inverse-albedo as reflectance of a true scene. This is shown in Fig. 2.

4 Visibility restoration algorithm

4.1 Atmosphere color estimation

To calculate $\mathbf{B}(\mathbf{x})$, airlight color $\mathbf{L}_\infty$ should be estimated at first. There are some methods to solve this problem. Nayar [16] introduced a method to estimate L_∞ by averaging a patch of the sky on the foggy image. This method could achieve good estimation and was used in some following algorithms [12, 20]. However, it merely works with sky in the scene. Fattal [8] and Narasimhan [15] calculated direction of $\mathbf{L}_\infty$, but the intensity is hard to be determined.[1] Tarel [21]

[1] Fattal [8] also gave a method to determine the intensity of $\mathbf{L}_\infty$, but this method can only work on his assumption.

Fig. 3 Synthetic experiment. This experiment shows that our method can work properly on well-texture images. (**a**) Original image. (**b**) Synthetic transmission. (**c**) Synthetic foggy image. (**d**) The transmission calculated by applying only Gaussian filter on $\mathbf{B}(\mathbf{x})$ ($w_1 = 15, \sigma_s = 5$). (**e**) The final result using (**d**). (**f**) The transmission obtained by applying 3-iteration bilateral filter on foggy image. (**g**) The final output image

estimated airlight $\mathbf{L}_\infty$ by calibrating white balance of the image. This method is simple to operate and works well for most of practical scenes. For universal usage consideration, we adopt white balance method to estimate $\mathbf{L}_\infty$ in our dehazing algorithm. $\mathbf{L}_\infty$ is set to be $[1, 1, 1]^{\mathrm{T}}$ after white balance is calibrated.

4.2 Initial transmission map extraction

$\mathbf{B}(\mathbf{x})$ can be calculated from $\mathbf{B}(\mathbf{x})$ definition equation when $\mathbf{L}_\infty$. A basic idea to separate the transmission from $\mathbf{B}(\mathbf{x})$ is to blur the image with a low-pass Gaussian filter $G(w, \sigma_s)$, with variance σ_s and window size w_1. If p and q are pixel locations, we have

$$B_{\mathrm{init}}(p) = \frac{\sum_q G(p, q, w_1, \sigma_s) B(q)}{\sum_q G(p, q, w_1, \sigma_s)}. \tag{4}$$

The size and the variance of the Gaussian filter are dependent on the local "feature" size S_{feature}. In practice, we just set $\sigma_s = S_{\mathrm{feature}}$.[2] After applying this Gaussian filter on $\mathbf{B}(\mathbf{x})$, only large-scale transmission variations and the color information remain. Although $B_{\mathrm{init}}(\mathbf{x})$ is *not* the true transmission, the difference between $B_{\mathrm{init}}(\mathbf{x})$ and $B_{\mathrm{init}}(\mathbf{y})$ can be an indicator of the similarity between $t(\mathbf{x})$ and $t(\mathbf{y})$, where $\mathbf{x}$ and $\mathbf{y}$ are pixels in a small local window. So we call $B_{\mathrm{init}}(\mathbf{x})$ a *similarity map*. We *do not* treat $B_{\mathrm{init}}(\mathbf{x})$ as true transmission values, but take the differences of its elements as a range Gaussian's input to apply bilateral filter to $B(\mathbf{x})$ in the next step.

4.3 Edge-preserved transmission map iteration

As shown in Figs. 3 and 4, there is an obvious deficiency in the recovered image in the discontinuities of the transmission map. Figures 3(d) and 3(e) show that only Gaussian filter may generate deficiency in the final output image.

In order to handle this discontinuities, we adapt *iterative bilateral filter* to our algorithm. It is an iterative method, and the current estimation of the transmission is used to drive the range Gaussian. The process can be summarized as

$$\begin{aligned} B_{i+1}(\mathbf{p}) &= \frac{\sum_q K(\mathbf{p}, \mathbf{q}) B(\mathbf{q})}{\sum_q K(\mathbf{p}, \mathbf{q})}, \\ K(\mathbf{p}, \mathbf{q}) &= G(\mathbf{p}, \mathbf{q}, w_2, \sigma_s') G(B_i(\mathbf{p}), B_i(\mathbf{q}), w_2, \sigma_r), \end{aligned} \tag{5}$$

where σ_r is the variance of the range Gaussian, σ_s' is the variance of the spacial Gaussian, and their windows are both w_2. These two parameters describe the influence that the pixels in the local window impose on the center pixel. They control the smoothness of the transmission map. In our algorithm, σ_r is an iteration-relevant variable. It has been proven in practice that $\sigma_{r_{i+1}} = 0.5\sigma_{r_i}$ can generate a good result. The initial σ_r is always set in $[0.08, 0.3]$. σ_s' is always smaller than the initial σ_s, and it depends on the resolution of the original image. The main difference between this approach and standard bilateral filter is that we always filter the initial image $\mathbf{B}(\mathbf{x})$. Because the kernel averages only pixels of similar estimated transmission, the filter can capture the transmission boundary.

This iteration process converges quickly and in practice it will converge after 3- or 4-times iteration. We define the last output of (5) as $B_{\mathrm{end}}(\mathbf{x})$. $B_{\mathrm{end}}(\mathbf{x})$ contains the transmission information and the averaged color information from $\mathbf{C}(\mathrm{x})$.

4.4 Final transmission extraction and visibility restoration

When we get $B_{\mathrm{end}}(\mathbf{x})$ using the iterative method described above, it contains color information which comes from inverse-albedo. In order to obtain true transmission, we must wipe out this color information. We first consider a simple case where $\rho(\mathbf{x})$ is a well-textured image.

If the foggy image is a well-textured image, so are $\mathbf{C}(\mathbf{x})$ and $\mathbf{B}(\mathbf{x})$. Since we apply (5) on $\mathbf{B}(\mathbf{x})$, the texture color is averaged. This averaged color comes from the $\mathbf{C}(\mathbf{x})$ component, so we just divide $B_{\mathrm{end}}(\mathbf{x})$ by the averaged color to obtain the $t(\mathbf{x})$. We have done a synthetic experiment, whose results are shown in Fig. 3.

However, natural image are not all well textured. But in a local window we can regard it as something like texture in some way. So for natural images, the color information

[2] S_{feature} can be easily seen in the input image, and so it is set by the user.

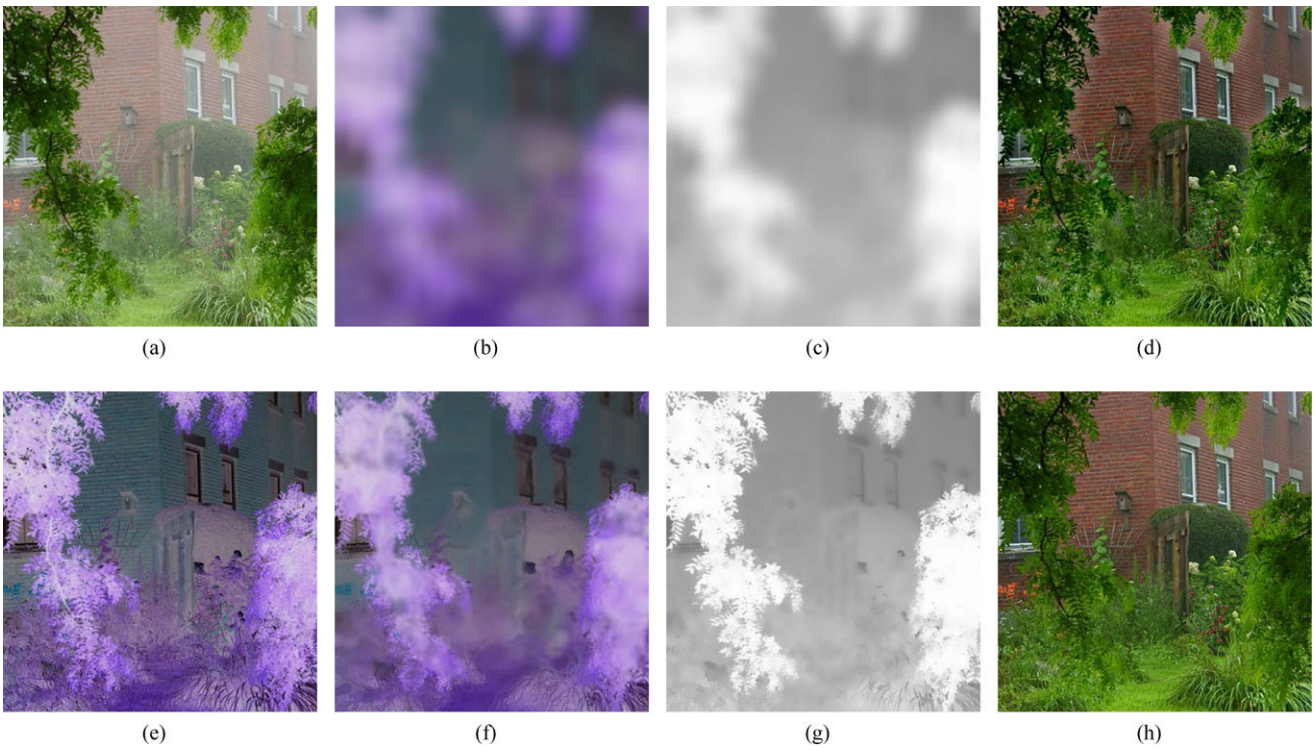

Fig. 4 True example. (**a**) Input image. (**b**) Gaussian blur on (**e**). (**c**) Transmission obtained by (**b**). (**d**) Output image using (**c**). (**e**) $B_{\text{init}}(\mathbf{x})$ ($\sigma_s = 6$, $w_1 = 21$). (**f**) Bilateral filter to (**b**) (with $\sigma_s' = 10$, $\sigma_r = 0.08$). (**g**) Transmission obtained by (**f**). (**h**) The final restored result

residual in $B_{\text{end}}(\mathbf{x})$ in a local window does not come from the whole averaged color of $C(\mathbf{x})$, but from a local area of the image. Since $B_{\text{end}}(\mathbf{x})$ has been blurred, the texture-detail cannot be distinguished. So we just divide $B_{\text{end}}(\mathbf{x})$ into groups according to the chromaticity-similarity. We project $B_{\text{end}}(\mathbf{x})$ into YUV color space and extract a single chroma based on the ratio of these projections:

$$\theta(\mathbf{x}) = \tan^{-1}(U/V). \tag{6}$$

This maps pixel color into angles where we measure distance by the length of the shortest arc, i.e.,

$$\text{dis}(\theta_1, \theta_2) = \min(|\theta_1 - \theta_2|, 2\pi - |\theta_1 - \theta_2|). \tag{7}$$

According to the pixel color distance defined by (7), we separate $B_{\text{end}}(\mathbf{x})$ into M groups, where M is a parameter set by the user according to the color variety. A true image experiment is shown in Fig. 4. The synthetic experiments shown in Fig. 3 can demonstrate the effect on this filter. Although there is a clear edge in transmission, the iterative bilateral filter can extract the low-frequency information and preserves the edges.

When the transmission is obtained, the inverse-albedo can be obtained by dividing the $\mathbf{B}(\mathbf{x})$ by $t(\mathbf{x})$, and then the albedo can be calculated. By multiplying the albedo by the atmosphere color, we can get the fog-free image.

5 Results and applications

We have done several experiments, including true scenes and synthetic scenes, working on color images and gray ones, to demonstrate our method can generate good results.

Figure 5 shows the comparison with [12]. The visibility restored by [12] is high-colored and make people feel unrealistic. The main reason is that the depth map recovered by Kratz [12] contains reductant details which may be wrong. For example, we regard the red bricks and the slots between them share the same depth values, so you should *NOT* differentiate between each other. However, as shown in Fig. 5(d), you can easily see the slots between the bricks in transmission map estimated by Kratz [12]. In our transmission map, the redundant details have been successfully removed, which makes the results better than [12].

Our algorithm can also work well on gray level foggy image. Figure 6 shows the result of applying our result on gray-level image.

Figure 7 shows the results of our method compared with [10]. The variance of spacial Gaussian $\sigma_s = 15$ and range Gaussian $\sigma_r = 0.2$ is used for our result. Kopf et al. [10] utilize the 3D model to remove haze, so we regard its result as the ground truth. We compare our results with the ground truth. From these images we can see that although

the result we get is not as good as the ground truth, it enhanced the contrast according to spatial variance.

Figure 8 shows the result using the Tan's [20] photo. This photo contains more details, and depth varies sharply between these details. So we must have a relative small σ_r to insure that the transmission is calculated by itself, otherwise the transmission map may lose some details.

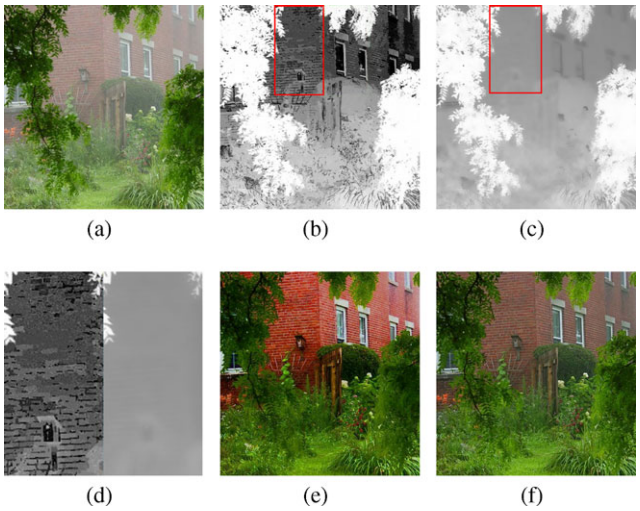

Fig. 5 Compare our result with [12] using the yard image provided by [8]. (**a**) Input image. (**b**) Transmission in Kratz [12]. (**c**) Our transmission. (**d**) Zoom in comparison. (**e**) Result in Kratz [12]. (**f**) Our result

Fig. 6 Our method working on gray scale image. (**a**) Foggy image. (**b**) Defogged image by our method

Applications. After having the transmission map $t(\mathbf{x})$, we can calculate the scene depth $d(\mathbf{x}) = \frac{\ln t(\mathbf{x})}{-\beta}$.[3] Then we can add more visual effect on the fog-free image, such as relighting or refocusing. Figure 9 shows the additional effects on the fog-free images.

6 Conclusion and future work

In this paper, we present a novel method based on bilateral filter for removing haze from single image. This method is based on the assumption that only the variation of transmission can result in large-scale luminance variation in the fog-free image. In other words, transmission is a low-frequency variable comparing to the fog-free image. We then use Gaussian filter to separate the low-frequency variables from the mixed signals. However, only Gaussian filter may not generate satisfactory result. So we apply a bilateral filter on the mixed signals, with the image previously obtained as a range Gaussian, to make sure that the edges are preserved.

For future work, we intend to concentrate on the current constraints of our method. Although our method can deal with most fog-picture, it will fail in case our assumption does not hold. If we meet with an image with large-scale atmosphere-color-like object, this method cannot calculate the transmission map correctly. It is because in the process of decolorizing we described in Sect. 4.4, the averaged colors are estimated from the $\mathbf{B}(\mathbf{x})$, which will suffer more errors when $\rho(\mathbf{x})$ approaches L_∞. For some small areas of white, this error can be averaged by the pixels around it, while it is not possible for large white areas. However, if the depth in the image varies sharply at the same time, our method may generate a bad result. Figure 10 shows a failed example. You can see that the transmission of the square is not calculated properly. Of course, tuning σ_r small is a way

[3] Here, we must provide the scattering coefficient β as a parameter. In most time, it is a value between 1.0–3.0.

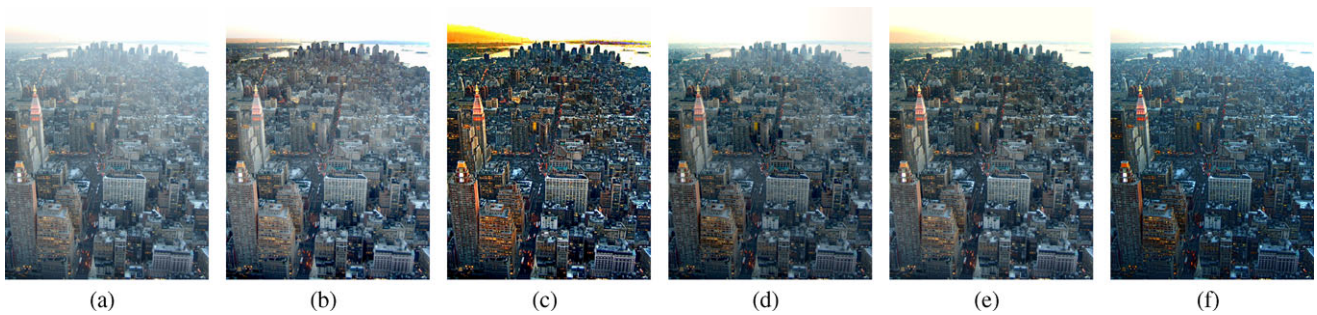

Fig. 7 The comparison between recent dehazing work. Left to right are: Input image, the result obtained by Kopf et al. [10], Tan [20], Fattal [8], He et al. [9], and our result

(a) (b) (c) (d)

Fig. 8 The comparison using Tan [20] as input. One can see that there is too much detail in the image, so we must set a small σ_r. (**a**) Input. (**b**) The result of Tan [20]. (**c**) The result of Kratz. (**d**) Our result ($\sigma_r = 0.04$)

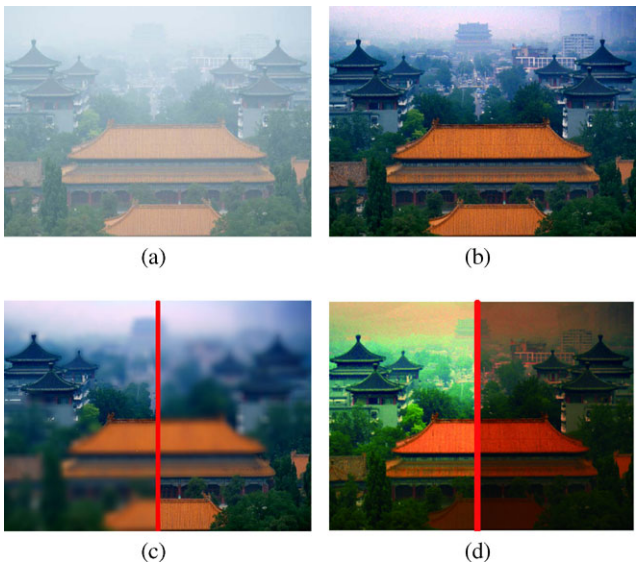

(a) (b) (c) (d)

Fig. 9 Additional application based on the depth map. (**a**) Input image. (**b**) Recovered image. (**c**) Refocused. *Left*, focus at middle of the image; *Right*, focus at near of the image. (**d**) Relighting result. *Left*, cloudy effect; *Right*, rosy dawn

(a) (b) (c)

Fig. 10 Failure example. (**a**) Input image. (**b**) Dehazed image. (**c**) Transmission map. One can see that the transmission in the square is not calculated properly

to solve this hole, but the transmission we obtained by this way is not correct.

References

1. Aleksic, M., Smirnov, M., Goma, S.: Novel bilateral filter approach: Image noise reduction with sharpening. In: Proceedings of SPIE—The International Society for Optical Engineering, vol. 6069, pp. 114–241. San Jose, CA, United States (2006). doi:10.1117/12.643880
2. Aurich, V., Weule, J.: Non-linear Gaussian filters performing edge preserving diffusion. In: Mustererkennung 1995, 17. DAGM-Symposium, pp. 538–545. Springer, London (1995)
3. Barash, D., Comaniciu, D.: A common framework for nonlinear diffusion, adaptive smoothing, bilateral filtering and mean shift. Image Vis. Comput. **22**(1), 73–81 (2004). doi:10.1016/j.imavis.2003.08.005
4. Bennett, E.P., McMillan, L.: Video enhancement using per-pixel virtual exposures. ACM Trans. Graph. **24**, 845–852 (2005). doi:10.1145/1073204.1073272
5. Durand, F., Dorsey, J.: Fast bilateral filtering for the display of high-dynamic-range images. ACM Trans. Graph. **21**, 257–266 (2002). doi:10.1145/566654.566574
6. Eisemann, E., Durand, F.: Flash photography enhancement via intrinsic relighting. ACM Trans. Graph. **23**, 673–678 (2004)
7. Elad, M.: On the origin of the bilateral filter and ways to improve it. IEEE Trans. Image Process. **11**(10), 1141–1151 (2002). doi:10.1109/TIP.2002.801126
8. Fattal, R.: Single image dehazing. ACM Trans. Graph. **27**(3), 1–9 (2008). doi:10.1145/1360612.1360671
9. He, K., Sun, J., Tang, X.: Single image haze removal using dark channel prior. In: 27th IEEE Conference on Computer Vision and Pattern Recognition, CVPR, pp. 1956–1963 (2009)
10. Kopf, J., Neubert, B., Chen, B., Cohen, M., Cohen-Or, D., Deussen, O., Uyttendaele, M., Lischinski, D.: Deep photo: Model-based photograph enhancement and viewing. ACM Trans. Graph. **27**(5) (2008)
11. Koschmeider, H.: Theorie der horizontalen sichtweite. Beitr. zur Phys. d. freien Atm. 171–181 (1924)
12. Kratz, L., Nishino, K.: Factorizing scene albedo and depth from a single foggy image. In: Proceedings of IEEE Twelfth International Conference on Computer Vision ICCV'09, pp. 1701–1708 (2009)
13. Liu, C., Freeman, W.T., Szeliski, R., Kang, S.B.: Noise estimation from a single image. In: Proceedings – 2006 IEEE Computer Society Conference on Computer Vision and Pattern Recognition, CVPR 2006, vol. 1, pp. 901–908. New York, NY, USA (2006). doi:10.1109/CVPR.2006.207
14. Narasimhan, S.G., Nayar, S.: Interactive deweathering of an image using physical models. In: IEEE Workshop on Color and Photometric Methods in Computer Vision, In Conjunction with ICCV (2003)
15. Narasimhan, S.G., Nayar, S.K.: Chromatic framework for vision in bad weather. In: Proceedings of the IEEE Computer Society Conference on Computer Vision and Pattern Recognition, vol. 1, pp. 598–605. Hilton Head Island, SC, USA (2000)
16. Nayar, S.K., Narasimhan, S.G.: Vision in bad weather. In: Proceedings of the IEEE International Conference on Computer Vision, vol. 2, pp. 820–827. Kerkyra, Greece (1999)

17. Oh, B.M., Chen, M., Dorsey, J., Durand, F.: Image-based modelling and photo editing. pp. 433–442. Los Angeles, CA, USA (2001)
18. Paris, S., Durand, F.: A fast approximation of the bilateral filter using a signal processing approach. Int. J. Comput. Vis. **81**(1), 24–52 (2009). doi:10.1007/s11263-007-0110-8
19. Schechner, Y.Y., Narasimhan, S.G., Nayar, S.K.: Instant dehazing of images using polarization. In: Proceedings of the IEEE Computer Society Conference on Computer Vision and Pattern Recognition, vol. 1, pp. 1325–1332. Kauai, HI, United States (2001). ISSN 10636919
20. Tan, R.T.: Visibility in bad weather from a single image. In: 26th IEEE Conference on Computer Vision and Pattern Recognition, CVPR. Anchorage, AK, USA (2008). doi:10.1109/CVPR.2008.4587643
21. Tarel, J.P., Hautière, N.: Fast visibility restoration from a single color or gray level image. In: Proceedings of IEEE International Conference on Computer Vision (ICCV'09), pp. 2201–2208. Kyoto, Japan (2009)
22. Tomasi, C., Manduchi, R.: Bilateral filtering for gray and color images. In: Proceedings of the 1998 IEEE 6th International Conference on Computer Vision, 4–7 January 1998, pp. 839–846. IEEE, Bombay, India (1998)
23. Winnemoller, H., Olsen, S.C., Gooch, B.: Real-time video abstraction. ACM Trans. Graph. **25**, 1221–1226 (2006). doi:10.1145/1141911.1142018

Jiawan Zhang received the M.Phil. and Ph.D. degrees in computer science from The Tianjin University in 2001 and 2004, respectively. Currently, he is an Associate Professor in the School of Computer Software and Adjunct Professor in the School of Computer Science and Technology, Tianjin University. His main research interest is scientific visualization, information visualization, visual analytics, medical image processing, and image synthesis. He is a member of the ACM and IEEE.

Liang Li received the B.S. degree in the School of Computer Science and Technology from Dalian University of Technology, P.R. China, in 2008. He is currently working toward the Ph.D. degree in computer application at the Graphics And Visual Computing Laboratory, Tianjin University. His main research interests include computer vision and information visualization.

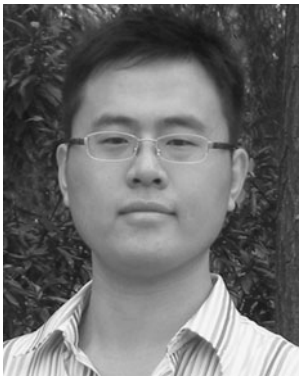

Guoqiang Yang received the B.S. degree in the School of Computer Science and Technology from Hebei University of Technology, P.R. China, in 2008. He is currently working toward the B.S. degree in computer application at the Graphics And Visual Computing Laboratory, Tianjin University. His main research interests include Computer Vision and Information visualization.

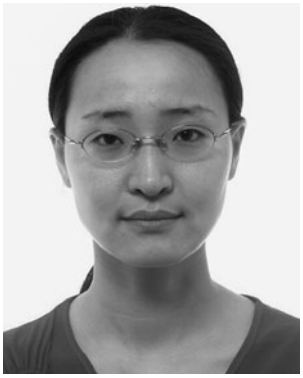

Yi Zhang received Master and Ph.D. degrees in computer science from Tianjin University in 2006 and 2009, respectively. She joined the Department of Computer Science and Engineering at Tianjin University at March 2009, where she is currently a lecturer. Her research interests include image editing, image style, virtual heritage restoration, and information visualization.